MEMS Technology for Optical Crosslink for Micro/Nano Satellites

W. Piyawattanametha, L. Fan*, S. S. Lee, John G. D. Su and M. C. Wu

Department of Electrical Engineering, University of California, Los Angles
66-147D Engineering IV, 405 Hilgard Ave., Los Angeles CA 90095-1594, USA
Tel: 310-825-7338, Fax: 310-794-5513, Email: wu@ee.ucla.edu
*Optical Micro-Machines, Inc., 6160 Lusk Blvd., Suite C-105, San Diego, CA 92121, USA

Abstract

We report on a novel, compact two-dimensional (2D) scanning micromirror for free space optical crosslinks for micro and nano satellites. Using a novel micromachined structure called Micro-Elevator by Self-Assembly (MESA) [1], the micromirror is suspended above the substrate by several hundred micrometers. Large mirror size and wide scanning range are achieved simultaneously. Large number of resolvable spots (>100) can be realized. Experimentally, optical scanning angles of ±14° have been achieved for the 2D scanner with mirror size of 400 μm × 400 μm. The resonant frequencies are around 500 Hz.

Introduction

Free-space optical crosslinks offers unprecedented connectivity and link capacity for communication among satellites. Pointing and tracking (P/T) of the optical beams are one of the most challenging tasks for this application. Conventional systems employ motorized gimbles, which are bulky, heavy, and expensive. The Micro-Electro-Mechanical-Systems (MEMS) technology offers a revolutionary approach to implement compact and light weight P/T systems for micro and nano satellites. Two-dimensional (2D) optical scanners with large rotation angles, narrow beam divergence, and high resonant frequency are the key components for the P/T systems.

Two-dimensional optical scanner can be realized by combining two one-dimensional (1D) scanners with orthogonal axes or using a single micromirror with two degrees of freedom. Several surface-micromachined 1D scanners have been reported [2-4]. The combinations of two cascaded 1D scanners have been demonstrated by M. H. Kiang, et al. [4] and P. Hagelin, et al. [5]. However, the cascaded 1D scanners have several disadvantages. The optical beams moves across the second mirror as the first mirror scans. As a result, either a large second mirror or some imaging optics is needed for large scan angles. The former results in low resonant frequency, while the latter makes it more difficult to monolithically integrate the 2D scanners. The 2D scanner using a single mirror with two degrees of freedom are therefore more desirable. Previously, several 2D Scanners have been reported [6,7]. To achieve a large number of resolvable spots for the 2D scanner, large separation between the micromirror and the substrate is required. This can be achieved by etching the substrate [6] or wafer bonding technique [7]. Though standard surface-micromachining offers many advantages and flexibility, most of the 2D scanners to date can only achieve a very limited number of resolvable spots.

In this paper, we report a novel surface-micromachined 2D optical scanning micromirror fabricated by the standard surface-micromaching process offered by MCNC [8]. This micromirror has a large mirror size, large scanning angles, and small actuation voltage. It is based on the MESA structure, which allows large micromirrors to be suspended at several hundreds micrometers above the substrate. The micromirror has an area of 400 μm × 400 μm.

Design and Fabrication

The schematic drawing of the 2D optical scanning micromirror is illustrated in Fig. 1. A nested torsion mirror is attached to a fixed polysilicon frame supported by the MESA structure. The MESA consists of five hinged polysilicon plates. The two outer plates are connected to in-plane micro actuators. As the microactuators move towards each other, the center plate will buckle up and rise above the surface of the substrate. The height is defined by the length of the side support plates, and can be made as high as several millimeters. Torsion mirrors as large as 5 mm x 5 mm have been successfully suspended by the MESA structure.

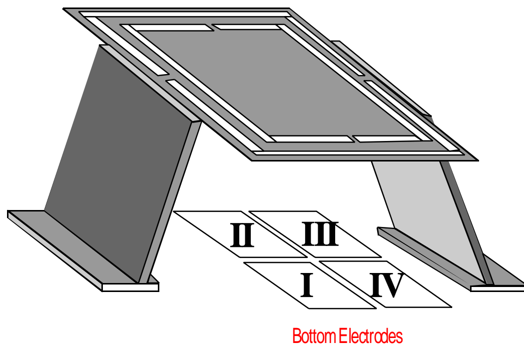

Figure 1: Schematic of 2D scanning micromirror realized by MESA.

The micromirror is attached to a pair of suspended frames through two sets of orthogonal torsion beams. The micromirror can be rotated around two axes by applying electrostatic force between the mirror and the quadrant electrodes on the substrate.

The self-assembly and operation of the micromirror is illustrated in Fig. 2. For simple illustration, only two side support plates are drawn. The basic structure consists of three parts: the micromirror platform, the side support plates, and scratch drive actuator (SDA) arrays [9]. The plates are joined together by polarity hinges. These hinges join two polysilicon plates together and allow them to bend only in one direction (either upwards or downwards). Details of the polarity hinges have been described in [1]. The 2D scanner can be fully assembled by applying electrical bias to the SDA arrays [9] attached to the outer plates. The side support plates with polarity hinges effectively translate the in-plane motion into out-of-plane motion, which in turn raise the platform, as illustrated in Fig. 2 (b).

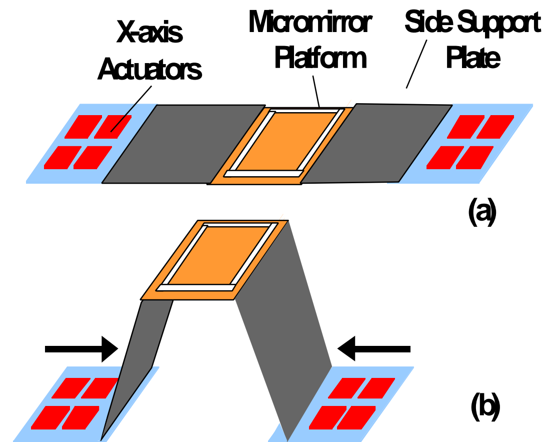

Figure 2 : Schematic diagrams illustrating the principle of the self-assembled micromirror (a) before assembly, (b) micromirror after assembly.

Figure 3 shows the scanning electron micrograph (SEM) of the 2D scanner. To improve the stability of the fixed frame, the MESA is supported from four sides.

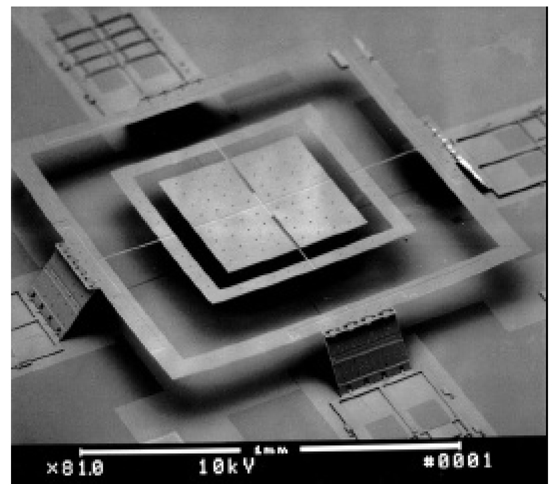

Figure 3: SEM of the 2D scanner.

Electrical Biasing and Controlling Scheme

The micromirror (400 μm x 400 μm) is attached to the fixed frame by torsion beams and suspended over four electrodes. The height of the structure is set to be 72 μm above the electrodes. The torsion beams are 2 μm and 3 μm wide for the inner and the outer frames, respectively, 200 μm long, and 1.5 μm thick. The 2D scanner is biased electrostatically by the quad-electrodes in the analog regime before snap-down. By applying voltage bias to electrode I and II, the mirror is rotated around the Y-axis (Fig. 5 (a)). The mirror is rotated around X-axis when applying electrical bias to electrode II and III (Fig. 5 (b)).

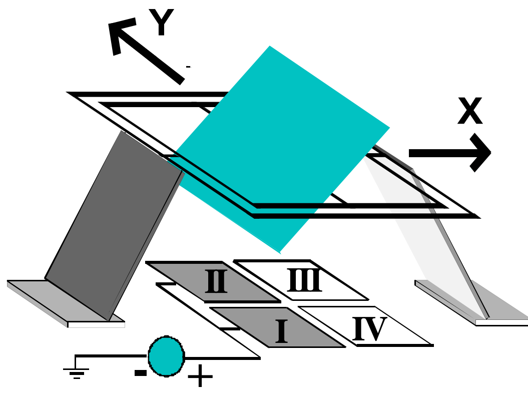

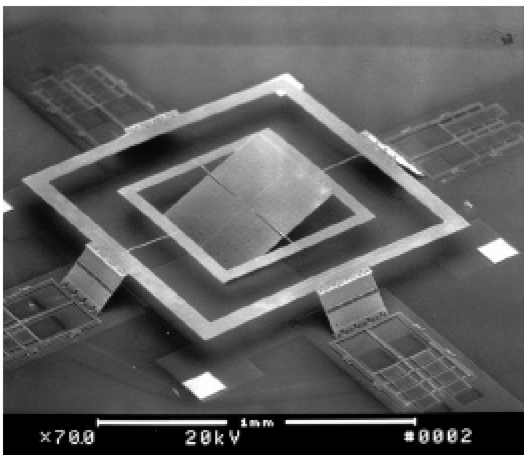

Figure 5 (a) : The mirror is rotated around the Y-axis.

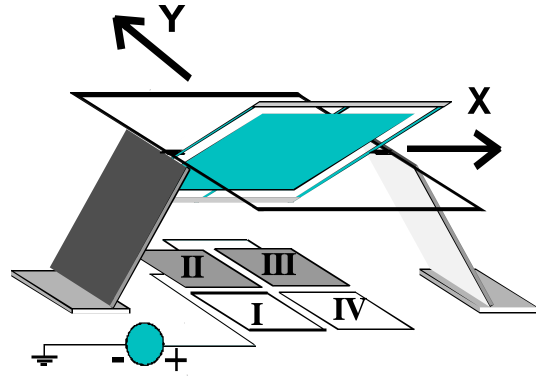

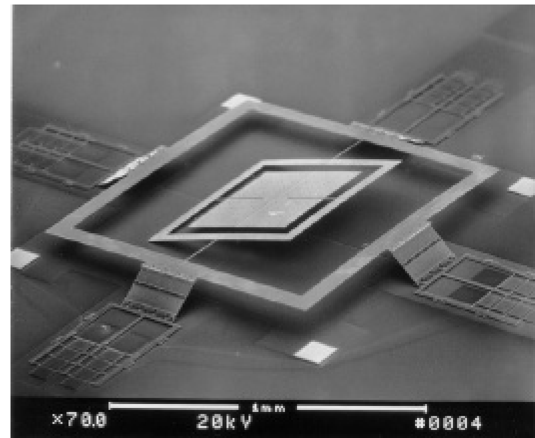

Figure 5 (b) : The mirror is rotated around the X axis.

For two-dimensional scanning, we divide the scanning pattern into four quadrants: Q1, Q2, Q3 and Q4. Fig. 6 (a) illustrates a triangle scanning pattern. It starts from point 1 to point 2, point 2 to point 3, and finally back to point 1 again. The variation of the mirror angles, θx and θy, versus time is illustrated in Fig. 6 (b).

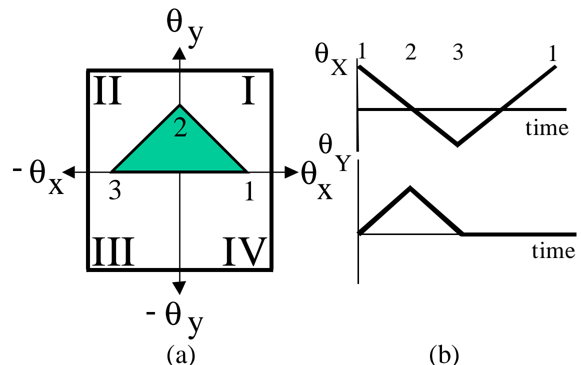

Figure 6 : (a) Triangle scanning pattern.
(b) Variation of the mirror angles, θx and θy, versus time .

When the mirror scans from point 1 to point 2, θx reduced from a positive value to zero while θy increased from zero to a positive value. Scanning from point 2 to point 3 and point 3 to point 1 can be realized by the same principle.

The mirror angles can be controlled by properly biasing the quad electrodes. Applying a voltage bias on electrode I will tilt the mirror in the +θx and +θy direction, Q1. Similarly, biasing electrode II, III, and IV will tilt the mirror in Q2, Q3, and Q4, respectively. Arbitrary scanning pattern is obtained by supplying proper waveforms to the quad electrodes. We use a computer controlled programmable waveform generator to supply the biases for all the electrodes. Fig. 7 shows the biasing waveforms for scanning a triangle pattern.

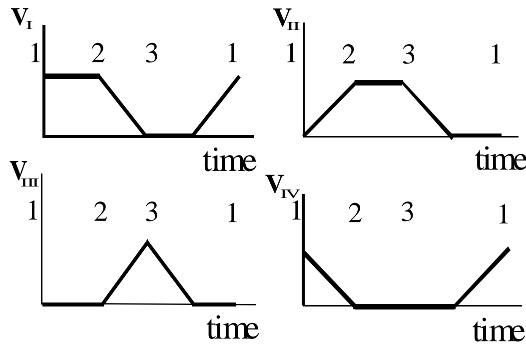

Figure 7 : Waveform patterns for each electrode.

The experimental setup for testing the 2D scanner is shown in Fig. 8. The system is composed of a 0.8 mW He-Ne laser operating, a fiber optic collimator, an imaging lens, a CCD camera, and a computer-controlled arbitrary waveform generator (National Instruments arbitrary waveform generators card AT-AO-10).

The He-Ne laser is used as the light source for this scanning system. The collimated light from the fiber collimator is projected directly onto the micromirror. The reflected beam from the micromirror is collected by the imaging lens before it falls on the CCD camera.

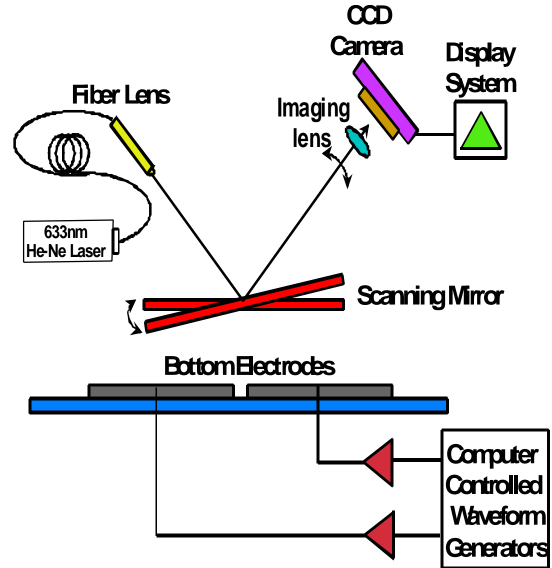

Figure 8 : Experimental setup of the scanning system.

Data from the experiment suggests that the spot size does not change appreciably as the mirror rotates. Displayed in Fig. 9 are four individual characters (UCLA) written by this laser scanning system to demonstrate the 2D scanning ability.

Figure 9 : Four characters (UCLA) displayed individually by the laser scanning system shown in Figure 8.

Mathematical Modeling

The structural parameter dependence of the yielding voltage was investigated by modeling the electrostatic torque on the mirror, as shown in Fig. 10 [10]. Two assumptions are made to simplify the calculation: 1) The distribution of the electrostatic field is uniform along the torsion beams, 2) The shape of the field is represented by the arc whose pivot is at the intersection, B, of the virtually extended mirror and the counter electrode.

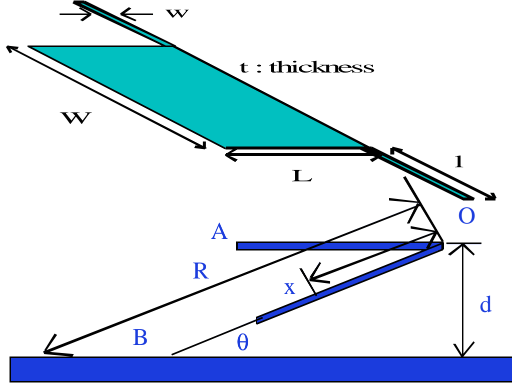

Figure 10 : Analytical model of the electrostatic torsion mirror.

When the mirror (W: width, L: length) is rotated inward by an angle θ, the length of BO is R=d/sin(θ), where d is equal to the height of micromirror structure. Since the length of the arc at x on the mirror is calculated a = d – xsin(θ), the magnitude of electrostatic field at x is

$$E = \frac{V}{d} = \frac{V}{d - x\sin\theta}, \qquad (1)$$

where V is the applied voltage. The electrostatic pressure on the surface is $P=\varepsilon E^2/2$, where $\varepsilon=8.85\times10^{-12}$ F/m is the dielectric constant of the vacuum. By integrating the electrostatic torque xPWdx over the electrode, we obtain the total torque by exerted electrostatic attraction

$$T_e = \frac{\varepsilon}{2} V^2 W \int_0^L \frac{x}{(d - x\sin\theta)^2}\, dx. \qquad (2)$$

On the other hand, the restoring torque of the torsion beams is

$$T_m = 2 \times \frac{Gwt^3\theta}{3l}\left\{1 - \frac{192t}{\pi^5 w}\tanh\left(\frac{\pi w}{2t}\right)\right\}, \qquad (3)$$

where G is the elastic constant of polysilicon. The resonant frequency of the torsion mirror is [11]

$$F_r = \frac{1}{2\pi r}\sqrt{\frac{Gwt^4}{6Ml}}. \qquad (4)$$

Experimental Results

From the experiment, we find the pull-in voltage and the resonant frequency of the outer and inner frames to be 104.8 V, 552 Hz and 94.5 V, 448 Hz, respectively. The optical deflection angle versus the applied voltage of the outer and the inner frames are illustrated in Fig. 11 (a) and (b), respectively. The measured data agrees well with the theoretically calculated data using 72 GPa for the elastic constant of polysilicon and setting the widths of the outer and inner frames to 2.95 µm and 1.9 µm respectively. However, the calculated angle at pull-in voltage is smaller than the experimental values. Fig. 12 (a) and (b) are the measured frequency responses.

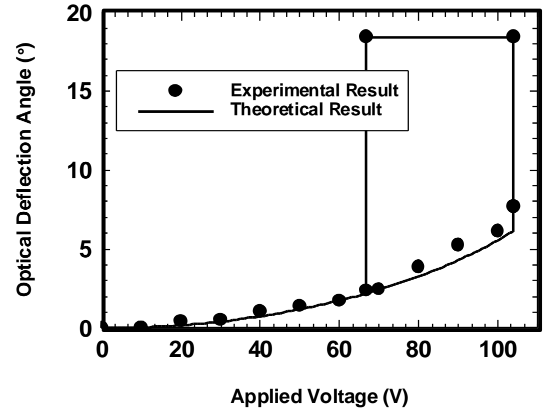

(a)

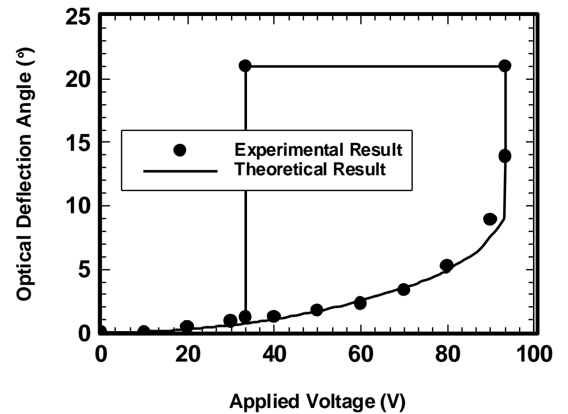

(b)

Figure 11 : (a) Optical Angle under applied voltage for outer frame.
(b) Optical angle under applied voltage for inner frame.

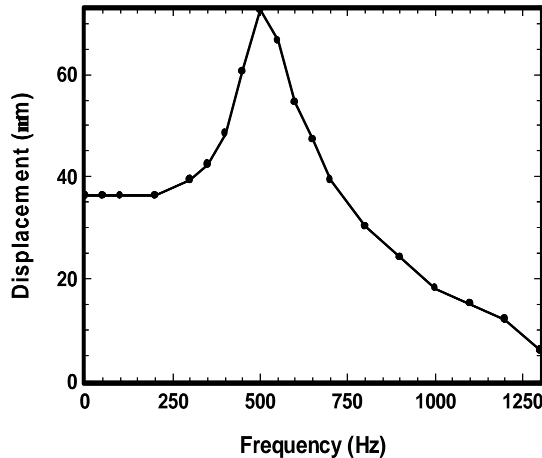

(a)

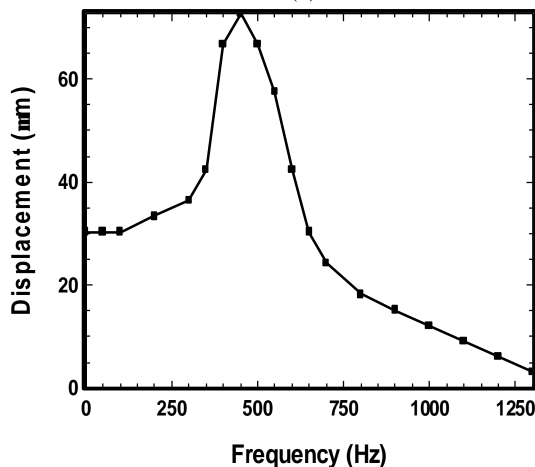

(b)

Figure 12 : (a) Frequency Response of the outer frame.
(b) Frequency Response of the inner frame.

The micromirror in this scanning system exhibit some curvature, resulting from stress gradients in the polysilicon film. Differences in curvature were found between identical devices on the same chip. Such anomalies are likely due to variations in the fabrication process.

Conclusion

We have demonstrated a novel self-assembled two-dimensional scanning micromirror using standard surface micromachining technology. Large optical deflection angles (±14 degrees for the inner frame and ±7 degrees for the outer frame) have been achieved for a 400 µm x 400 µm micromirror. The applications of this device include display, printing, optical data storage, optical scanning microscopes, and free-space optical links between satellites.

Acknowledgements

The author would like to thank Richard Chen, Thomas Jung, Andrew Rollinger, Sagi Mathai, and Hung Nguyen for technical assistance. This project is supported in part by DARPA.

Reference :

1. Li Fan, M. C. Wu, Kent D. Choquette, and Mary H. Crawford, "Self-assembled Microactuated XYZ Stages for Optical Scanning and Alignment," Proceedings of International Solid State Sensors and Actuators Conference (Transducers'97), Chicago, IL, USA, June 16-19, 1997, P. 319-322
2. S. S. Lee, and M. C. Wu, "Surface-Micromachined Vertical Torsion Mirror Switches," International Conference on Optical MEMS and their Applications (MOEMS'97), Nara, Japan, November 18-21, 1997, P. 85-88
3. G. D. Su, S. S. Lee, and M. C. Wu, " Out-of-Plane Vertical Torsion Mirror for Optical Scanner and Chopper Application," Conference on Lasers and Electro-Optics (CLEO'98), San Francisco, California, May 3-8, 1998 P. 479-480
4. M. H. Kiang, D. A. Francis, C. J. Chang-Hasnain, O. Solgaard, and K. Y. Lau, "Actuated Polysilicon Micromirrors for Raster-Scanning Displays," Proceedings of International Solid State Sensors and Actuators Conference (Tranducers'97), Chicago, IL, USA, June 16-19, 1997, P. 323-326
5. P. Hagelin, K. Cornett, and O. Solgaard, "Micromachined Mirrors in a Raster Scanning Display," IEEE/LEOS

Summer Topical Meeting, Monterey, California, July 20-24, 1998, P. 109-110

6. V. R. Dhuler, M. Walters, R. Mahadevan, A. B. Cowen, and K. W. Markus, "A Novel Two Axis Actuator for High Speed Large Angular Rotation," Proceedings of International Solid State Sensors and Actuators Conference (Tranducers'97), Chicago, IL, USA, June 16-19, 1997, P.327-330
7. W. Dotzel, T. Gessner, R. Hahn, C. Kaufmann, K. Kehr, S. Kurth, and J. Mehner, "Silicon Mirrors and Micromirror Arrays for Spatial Laser Beam Modulation," Proceedings of International Solid State Sensors and Actuators Conference (Transducers'97), Chicago, IL, USA, June 16-19, 1997, P. 81-84
8. MEMS Technology Applications Center at Microelectronics Center at North Carolina (MCNC), Research Triangle Park, North Carolina
9. A. Terunobu and H. Fujita, " A Quantitative Analysis of Scratch Drive Actuator Using Buckling Motion," Proceedings of IEEE Micro Electro Mechanical Systems, 1995, P. 310-315
10. H. Toshiyoshi, and H. Fujita, "Electrostatic micro-torsion Mirrors for an Optical Switch Matrix," Journal of Micro Electro Mechanical Systems, Vol. 5, No. 4, December 1996, P. 231-237
11. E. Hashimoto, Y. Uenishi, K. Honma, and S. Ngaoka, " Micro-optical gate for fiber optic communication," Proceedings of International Solid State Sensors and Actuators Conference (Transducers'97), Chicago, IL, USA, June 16-19, 1997, P. 331-334